Bifurcation-Like Behavior of Electrostatic Potential in LHD*)

Akihiro SHIMIZU, Takeshi IDO, Masaki NISHIURA, Ryohei MAKINO[1)], Masayuki YOKOYAMA, Hiromi TAKAHASHI, Hiroe IGAMI, Yasuo YOSHIMURA, Shin KUBO, Takashi SHIMOZUMA, Naoki TAMURA and LHD Experiment Group

National Institute for Fusion Science, 322-6 Oroshi-cho, Toki 509-5292, Japan
[1)]*Graduated School of Engineering, Nagoya University, Furo-cho, Chikusa, Nagoya 464-0814, Japan*

(Received 10 December 2012 / Accepted 26 June 2013)

The temporal evolution of the potential is measured with the heavy ion beam probe (HIBP) in the Large Helical Device (LHD). A rapid change in the potential is observed early in the tangential neutral beam injection (NBI) phase, just after the switch from tangential to perpendicular NBI, and in a low-power electron cyclotron heated (ECH) discharge in the LHD. The radial profile of the potential is measured before and after the potential change. This rapid potential change is considered to indicate the bifurcation of the radial electric field in the edge region of the LHD plasma.

Keywords: radial electric field, bifurcation, Heavy Ion Beam Probe, helical device

DOI: 10.1585/pfr.8.2402122

1. Introduction

The radial electric field E_r is an important parameter for studying the confinement physics of magnetically confined plasmas. The radial derivative of E_r drives the shear flow, which improves the confinement characteristics of the plasma for the suppression of turbulence. It is important to understand the formation physics of E_r to use the shear flow to realize good confinement properties. In helical devices, which have three-dimensional magnetic field configurations, E_r is determined mainly by the balance of non-ambipolar flux in the neoclassical context, and this field suppresses ripple diffusion in the $1/\nu$ regime. The positive E_r (so-called electron root) and negative E_r (ion root) are predicted theoretically in helical plasma [1]. The appearance of these roots depends on the profiles of the density, ion/electron temperature, and magnetic configuration. In some cases, both roots are predicted theoretically in some radial region, and bifurcation between these two roots is expected.

In the Large Helical Device (LHD), we have been studying the E_r formation physics in plasma using a heavy ion beam probe (HIBP) [2–5]. With this diagnostic system, we can directly measure the potential in high-temperature plasma with good spatial/temporal resolution. This report presents a resent experimental result of potential measurement in the LHD in which a rapid change in the potential is measured with the HIBP. This change is considered to be related to a bifurcation phenomenon. The typical time trace and potential profile are reported when this rapid change of potential is observed.

author's e-mail: akihiro@nifs.ac.jp

*) This article is based on the presentation at the 22nd International Toki Conference (ITC22).

2. Experimental Setup

The LHD is a heliotron device, the magnetic field configuration of which is characterized by the major radius of the magnetic axis R_{ax}, toroidal magnetic field strength B_t, pitch parameter γ and quadrupole component of the magnetic field B_q. The typical discharge reported here is obtained under the following conditions, $R_{ax} = 3.6\,\mathrm{m}$, $B_t = 1.5\,\mathrm{T}$, $\gamma = 1.254$, and $B_q = 100\%$. The averaged minor radius of the plasma is 0.6 m, and the typical line-averaged density and electron temperature in our experiment are $0.5 \sim 1.0 \times 10^{19}\,\mathrm{m}^{-3}$, and $0.5 \sim 1\,\mathrm{keV}$ respectively.

In the HIBP in the LHD, the tandem accelerator is employed to generate a maximum voltage of 3 MV. Negative ions (Au^-) are produced by the target sputtering ion source [6]. The Au^- beam is extracted and accelerated by a pre-accelerator to 64 keV. Thereafter, this beam is injected into the tandem accelerator and accelerated by the positive accelerator voltage. In a gas cell located at the center of the tandem accelerator, the Au^- ions are stripped of two electrons and changed to Au^+ ions. These ions are re-accelerated so the beam is accelerated twice by the accelerator voltage. The energy of the probe beam in the experiments reported here is 1.55 MeV. The probe beam is transferred through the beam line and injected into the plasma. The injection and ejection angles of the probe beam are controlled by eight-pole electrostatic deflectors at the injection and ejection ports. By controlling these angles, the observation point can be changed. The Au^+ ions of the injected probe beam (primary beam) are stripped of an electron by collisions with the plasma, and then gain potential energy at this ionization point. The energy of the produced Au^{2+} beam (secondary beam) is measured outside of the plasma by the energy analyzer. The difference

in energy between the injection and ejection beams corresponds to the plasma potential at the ionization point.

To detect the secondary beam current, microchannel plates (MCPs) were used. The order of the detected current is from a few tens of pA to a nA. The equilibrium value of the potential and its radial profile can be measured below the line averaged density of 1.5×10^{19} m^{-3}. However, the fluctuation measurement is possible only at low densities (below 0.5×10^{19} m^{-3}). At high densities ($> 2.0 \times 10^{19}$ m^{-3}), the attenuation of the probe beam in the plasma is strong, therefore, potential measurements with our present system are difficult.

3. Experimental Results of Neutral Beam Heated Plasma

The rapid change in the potential is measured with the HIBP in plasma heated by neutral beam injection (NBI). The typical wave form of the line-averaged density and heating methods are shown in Fig. 1 (a). Plasma is produced and sustained by tangential NBI heating (NBI#1 and NBI#2). The density increases just after the NB injection (3.3 s), and then decreases to $\sim 0.4 \times 10^{19}$ m^{-3}. The heating method is switched from tangential NBIs to perpendicular NBI (NBI#5). The line-averaged density increases after this switch. Additional electron cyclotron heating (ECH) is applied at 5.2 s, which reduces the line-averaged density. The time evolution of the potential at the center of plasma measured with the HIBP is shown in Fig. 1 (b). The potential at the center becomes positive in the tangential NBI phase (3.3 ~ 4.8 s), and it decreases to a small negative potential after the NB is switched from tangential to perpendicular. In the additional ECH phase, the potential again becomes positive because of low density and high electron temperature.

To investigate in more detail, the potential evolutions in Fig. 1 at the beginning of tangential NBI (3.45 ~ 3.55 s), just after the switching of the NB (4.80 ~ 4.90 s), and after the additional ECH is turned on (5.17 ~ 5.27 s) are shown in Figs. 2 (a), (b), and (c), respectively. In Fig. 2 (a), the potential gradually increases, and a rapid increase is observed at 3.478 s. In Fig. 2 (b), after the tangential NBs (NBI#2,#3) are turned off at 4.80 s, the potential gradually decreases, and a rapid decrease is observed at 4.856 s. In Fig. 2 (c), the potential gradually increases to positive just after the application of additional ECH (5.20 s). Rapid changes can be observed at 5.242 and 5.248 s. A rapid increase in the potential (forward change) is observed at a line-averaged density of 0.8×10^{19} m^{-3}, however, a rapid decrease of potential (backward change) is observed below 0.5×10^{19} m^{-3}. Regarding the density, the potential change exhibits hysteresis character. The typical time constant of these rapid potential changes is a few hundred micro to a few milliseconds. Figures 3 (a) and (b) show magnifications of Figs. 2 (b) and (c), respectively. The typical time constant is estimated using the fitting function of the hyperbolic tangent, $\Phi = \Phi_0 + a \times \tanh[(t - t_0)/\tau]$. In Fig. 3 (a), at 4.856 s, the time constant of the potential drop is 0.11 ms. In Fig. 3 (b), the time constants of the first and second increases in the potential are 0.29 ms and 1.1 ms, respectively. These are shorter than the confinement time (~20 ms), therefore, this rapid change is considered to be related to bifurcation phenomenon of the radial electric field. A similar bifurcation phenomenon was observed in CHS [7, 8], but the time constant of the potential change is 30 ~ 70 μs, which is shorter than that of the LHD.

The radial profile of the potential was measured with the HIBP, as shown in Fig. 4. This is not the same shot

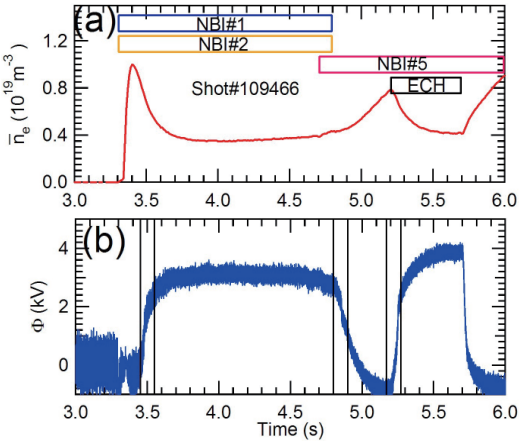

Fig. 1 (a) Typical wave form of line-averaged density and heating methods when the rapid change in potential is observed. (b) The time evolution of potential measured with HIBP.

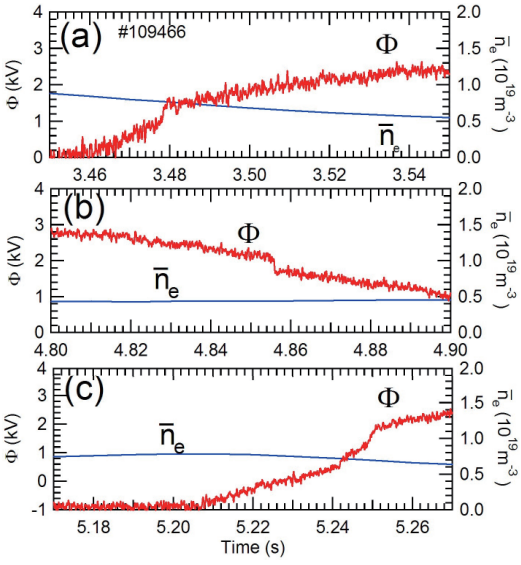

Fig. 2 Potential evolution in the beginning of tangential NB phase (a), just after the switch from tangential to perpendicular NB (b), and just after the additional ECH is applied (c).

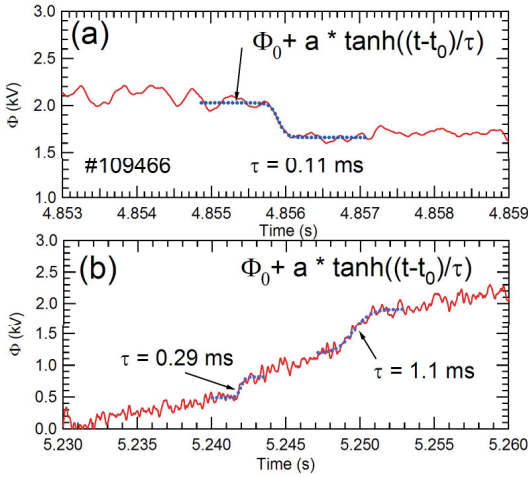

Fig. 3 Time expansion of potential evolution of Fig. 2 is shown. Figures 3 (a) and (b) corresponds to Figs. 2 (b) and (c), respectively.

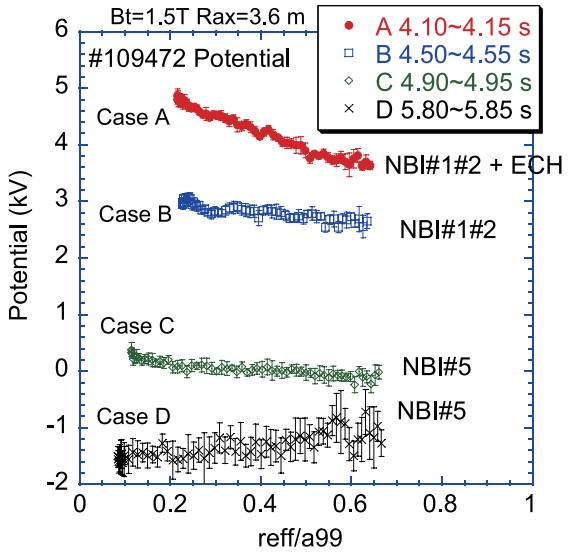

Fig. 4 Potential profiles in the phase of tangential NBI with additional ECH (Case A), tangential NBI (Case B), and perpendicular NBI (Cases C and D).

as in Figs. 1 and 2, but its plasma parameters are similar to those of the shot in Fig. 1. Only the timing of additional ECH is different: the ECH is applied at 5.2 - 5.7 s in Fig. 1, whereas it is applied at 3.9 - 4.4 s in this shot. The radial profiles of the potential in the phase of tangential NBI (NBI#1,#2) with additional ECH (Case A), tangential NBI (NBI#1,#2) (Case B), perpendicular NBI (NBI#5) just after the switch from tangential to perpendicular NBI (Case C), and perpendicular NBI (NBI#5) (Case D) are shown in Fig. 4. Here $r_{\rm eff}$ and a_{99} are the effective minor radius and that of the outermost flux surface, respectively. In this shot, the ECH resonance position is not at the center of the plasma, therefore, off-axis heating is applied, and temperature profile is relatively flat in the core region. No

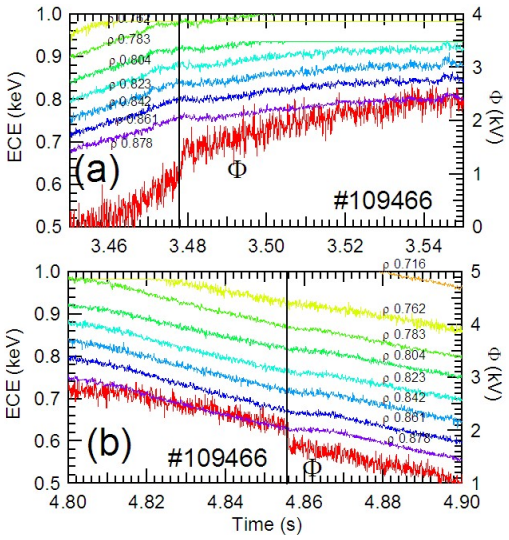

Fig. 5 Time evolutions of ECE when rapid potential change is observed. (a) in the beginning of tangential NBI and (b) just after the NB is switched.

internal transport barrier is observed in this shot. In Case A, a positive radial electric field is formed in the plasma, which is the so-called electron root in the neoclassical context. In Case B, a small positive radial electric field is observed in the core region, which is the so-called ion root. In Cases A and B, the tangential NBs sustain the plasma, and the large positive radial electric field in the outer region ($r_{\rm eff}/a_{99} > 0.7$) is deduced from experimental data, although the potential data cannot be obtained in this region owing to the limitations of the diagnostic port. In Cases C and D, the central potential becomes almost zero and negative, respectively. The radial electric field has a small positive or negative value in the entire radial region in Cases C and D. Even in the outer region ($r_{\rm eff}/a_{99} > 0.7$), the radial electric field is considered to be almost zero or slightly negative in these cases, and this $E_{\rm r}$ is the ion root. A rapid change in the potential occurs between Cases B and C. Bifurcation is considered to occur from the electron root to ion root in the outer region.

The time evolution of the electron cyclotron emission (ECE) signal is shown in Fig. 5 with the potentials at the beginning of tangential NBI (same as Fig. 1 (a)), and just after the NB is switched (same as Fig. 1 (b)). In Fig. 5 (a), the electron temperature gradually increases after the NB injection. At the time of rapid increase in the potential (3.478 s), the electron temperature stops increasing for a while. Subsequently, the electron temperature increases again, but the increase rate is less than that before potential transition. The plasma parameter is transient: therefore, the transport property is not clear, but the experimental result suggests that the transport properties of electrons before and after the potential transition differ. In Fig. 5 (b), the electron temperature gradually decreases with the potential. At the time of rapid decrease in the po-

tential (4.856 s), the electron temperature stops decreasing and remains at the same value for a while, after which it decreases. Transport property of electron is also changed by this potential transition.

4. Experimental Results of Low Power EC Heated Plasma

A rapid change in the potential is observed in the plasma sustained by low-power ECH (about 300 kW). The magnetic configuration is the same as that in Section 3, namely, R_{ax} = 3.6 m, B_t = 1.5 T, γ = 1.254, and B_q = 100%. The time evolution of potential, line-averaged electron density, and heating methods are shown in Fig. 6 (a). Figure 6 (b) is a time expansion of Fig. 6 (a). In Fig. 6 (b), the potential decreases as the density increases. A rapid decrease in the potential is observed at 3.655 s. Thereafter, back transition occurs. The time constant of the potential drop at 3.655 s estimated from a fitting function, $\Phi = \Phi_0 + a \times \tanh[(t - t_0)/\tau]$, is 0.1 ms, which is shorter than the energy confinement time (~30 ms). The time constant of the recovery phase from 3.655 s is about 0.93 ms, that is slower than the potential drop phase, but at 3.677 s, the time constant of the recovery phase is very short (~0.07 ms). Thus, the phenomenon is relatively complicated. After several forward and back transitions, the potential drops and sustains a gradual decrease. The radial potential profiles before (3.64 ~ 3.65 s) and after the transition (3.73 ~ 3.74 s) are shown in Fig. 7. These profiles are obtained from eight sequential shots, and the measurement point of the HIBP is changed shot by shot. The plasma parameters of these shots are similar, however, the timing of potential oscillation differs slightly. At 3.65 ~ 3.73 s, some shots of the potential are before the transition, but the others are after the transition: therefore, we do not show the profile in this phase. Note that the potential change due to the temporal change in the plasma parameters is included in Fig. 7. The potential in the entire radial region changes between before and after the transition, especially in the region where r_{eff} > 0.2 the radial electric field decreases with time.

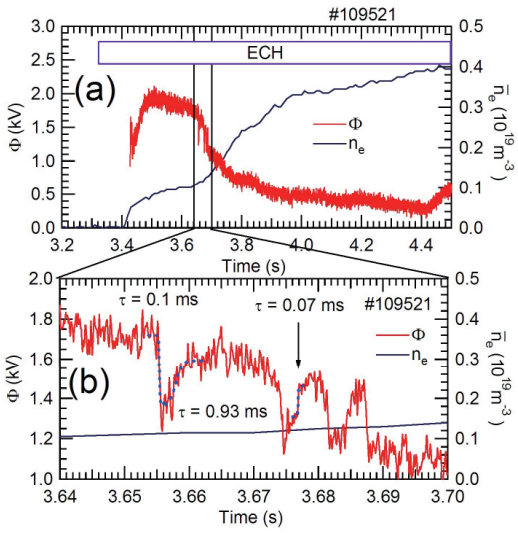

Fig. 6 Time evolutions of the potential in the low-power ECH discharge. Figure (b) shows a magnification of potential evolution (a).

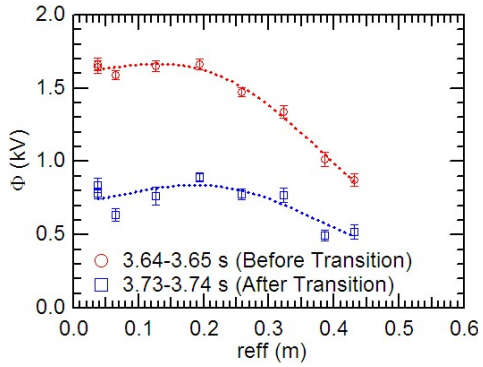

Fig. 7 Radial profile of the potential before and after the transition in the low power ECH discharge.

5. Summary

The temporal evolution of the plasma potential is measured with the HIBP in the LHD. A rapid change in the potential is observed at the beginning of tangential NB heating phase, after the switch from tangential NB to perpendicular NB, and in a low-power ECH discharge. The time constant of the potential change is roughly a few hundred μs, which is shorter than the confinement time, and this potential change is considered to be related to the bifurcation phenomenon of the radial electric field in the helical device. The time constant of the potential change in the LHD (100 μs ~ 1 ms) is longer than that in CHS (30 ~ 70 μs). A comparison with theory, such as neoclassical theory, is a future issue to investigate the mechanism of E_r formation in detail.

Acknowledgements

This work was supported by the NIFS budget under contract Nos. ULHH 020 and 023, and by JSPS KAKENHI Grant-in-Aid for Scientific Research (C) 24561031. The authors are grateful for the continuous support of the scientific and technical staff in the LHD experiments.

[1] M. Yokoyama *et al.*, Nucl. Fusion **42**, 143 (2002).
[2] F.C. Jobes, J.F. Marshall and R.L. Hickok, Phys. Rev. Lett. **22**, 1042 (1969).
[3] T. Ido, A. Shimizu, M. Nishiura, A. Nishizawa, S. Katoh, K. Tsukada, M. Yokota, H. Ogawa, T. Inoue, Y. Hamada *et al.*, Rev. Sci. Instrum. **77**, 10F523 (2006).
[4] A. Shimizu, T. Ido, M. Nishiura, H. Nakano, I. Yamada, K. Narihara, T. Akiyama, T. Tokuzawa, K. Tanaka *et al.*, J. Plasma Fusion Res. **2**, S1098 (2007).
[5] A. Shimizu, T. Ido, M. Nishiura, S. Nakamura, H. Nakano, S. Ohshima, A. Nishizawa, M. Yokoyama, Y. Yoshimura,

S. Kubo, T. Shimozuma, H. Igami, H. Takahashi, N. Tamura *et al.*, J. Plasma Fusion Res. **5**, S1015 (2010).
[6] M. Nishiura, T. Ido, A. Shimizu, S. Kato, K. Tsukada, A. Nishizawa, Y. Hamada, Y. Matsumoto *et al*., Rev. Sci. Instrum. **77**, 03A537 (2006).
[7] A. Fujisawa, H. Iguchi, H. Sanuki, K. Itoh, S. Lee, Y. Hamada, S. Kubo *et al*., Phys. Rev. Lett. **79**, 1054 (1997).
[8] A. Fujisawa, H. Iguchi, T. Minami, Y. Yoshimura, K. Tanaka, K. Itoh, H. Sanuki, S. Lee *et al*., Phys. Plasmas **7**, 4152 (2000).